

# Nonresonant transfer of excitation in He(2<sup>1</sup>S, 2<sup>3</sup>S) + Ne reactions

A. Z. Devdariani and A. L. Zagrebin

Leningrad State University

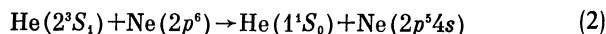
(Submitted 18 April 1983)

Zh. Eksp. Teor. Fiz. 86, 1969–1980 (June 1984)

Electron-atom scattering parameters and experimental data on He–Ne<sup>+</sup> interactions are used to calculate the He–Ne(*ns*) quasimolecular terms with  $n = 4$  and  $5$ . The calculated term values are supplemented by values deduced from differential scattering experiments. The data are then used to determine the coordinates of nonadiabatic regions and to establish mechanisms responsible for nonresonance excitation transfer leading to the population of different Ne\* states. The temperature dependence of the rate constants  $K(T)$  of the excitation-transfer reactions are related by a single integration to transition probabilities between the quasicrossing terms. Comparison between the calculated and experimental functions  $K(T)$  is used to determine the matrix elements of the interaction. The energy dependence of excitation cross sections is calculated for different neon states during excitation transfer.

## §1. INTRODUCTION. FORMULATION OF THE PROBLEM

There has been increased interest in the excitation-transfer reactions



since the advent of the first gas laser. They are now the most fully experimentally investigated nonresonant excitation-transfer processes.<sup>1</sup> Experimental data on the temperature dependence of the reaction rate constants  $K(T)$  and differential scattering cross sections have been interpreted in numerous recent papers in terms of different models of nonadiabatic transitions. Reaction (1) has been treated, for example, in terms of the optical model, the strong coupling method,<sup>2</sup> and the Landau-Zener model,<sup>3</sup> whereas reaction (2) has been interpreted in terms of the Demkov model<sup>4</sup> and the Landau-Zener model.<sup>5,6</sup> The use of this great variety of models for the interpretation of (1) and (2), frequently without preliminary justification of the validity of a particular model in relation to a given process, and the fact that the models are frequently mutually exclusive, suggests that the precise mechanism responsible for reactions (1) and (2) is still, to some extent, an open question.

The aim of this paper is to provide a theoretical analysis of reactions (1) and (2) by a method close to atomic collision spectroscopy.<sup>7</sup> A semiempirical term scheme for the system He–Ne( $2p^5ns$ ),  $n = 4, 5$  is constructed in Sec. 2 on the basis of data on the scattering of a weakly-bound electron, using the method proposed in Refs. 8 and 9, and the experimental data<sup>10</sup> on the He–Ne<sup>+</sup> interaction. This enables us to establish the reaction mechanisms and to determine the energy and radial coordinates of nonadiabatic regions. In Secs. 3 and 4, experimental data on  $K(T)$ , taken mainly from Ref. 4, 11, and 12, are compared with particular calculations of  $K(T)$ , which enables us to determine the off-diagonal matrix elements of the interaction.<sup>11</sup> This determination of the reaction mechanisms and interaction parameters enables us in Secs. 3 and 4 to provide a critical review of the mechanisms proposed in the literature, and to calculate the energy dependence of the reaction cross sections for (1) and (2). Experi-

mental studies of this energy dependence are difficult to perform, especially near the reaction threshold, which is particularly sensitive to the choice of the reaction mechanism. Moreover, the energy dependence is not only of interest in itself, but is also necessary for the solution of applied problems related to the optimization of different laser systems.

We shall use the atomic system of units in all our calculations.

## §2. THE He–Ne( $2p^5ns$ ), $n = 4, 5$ QUASIMOLECULAR TERMS

Preliminary analysis<sup>3,5</sup> has shown that nonadiabatic transitions in processes (1) and (2) occur for nuclear separations  $R$  smaller than the orbital radius of the excited  $s$ -electron in the neon atom. The nature of the He–Ne(*ns*) quasimolecular terms in this range of values of  $R$  is therefore largely determined by the ion-atom interaction.<sup>3</sup>

To construct the He–Ne(*ns*) terms, we shall take the Hamiltonian for the quasimolecule in the form

$$\hat{H} = \hat{H}_{\text{Ne}^*} + \hat{H}_{\text{He}} + \hat{V}_i + \hat{V}_e. \quad (3)$$

Here  $\hat{H}_{\text{He}}$ ,  $\hat{H}_{\text{Ne}^*}$  is the free-atom Hamiltonian, including the spin-orbit interaction that can be regarded as independent of  $R$  for the nonadiabatic transitions ( $R \gtrsim 4$ ) in which we are interested,<sup>13</sup>  $\hat{V}_i$  is the interaction potential between the Ne<sup>+</sup> ion and the He atom, and the operator  $\hat{V}_e$  represents the influence of the weakly-bound  $s$ -electron. The fact that the spin-orbit interaction in the quasimolecular ion is independent of  $R$  (Ref. 13) enables us to determine the matrix elements of the operator  $\hat{V}_i$ , using a procedure that is the converse of “turning on” the spin-orbit interaction<sup>14</sup> and the data<sup>10</sup> on the He–Ne<sup>+</sup> interaction. The matrix elements of  $\hat{V}_e$  were calculated by the method described in Refs. 8 and 9.

Figures 1 and 2 show the calculated He–Ne(*ns*) quasimolecular terms together with the  $1,3\Sigma^+ \text{He}(2^{1,3}S)$  terms,<sup>2</sup> deduced in Refs. 6 and 15 from scattering data, and the  $3d, 4p$  terms<sup>6</sup> (see the discussion given below). Allowance for the interaction between the calculated and measured terms of the same symmetry leads to a splitting in crossing regions. It will be established below that the characteristic size of the

$E \cdot 10^3$ , at.un.

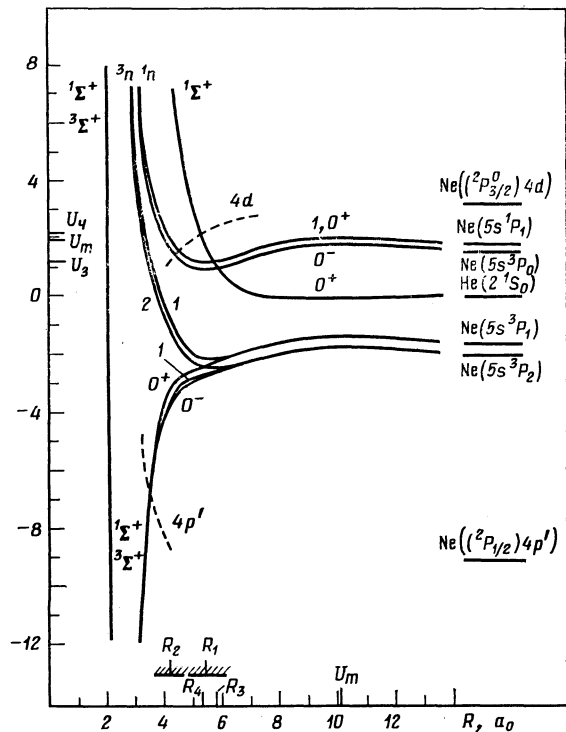


FIG. 1. The quasimolecular terms  $\Omega$   $\text{Ne}(5s^{1.3}P_J)$  (Sec. 2) and  $^1\Sigma^+ \text{He}(2^1S_0)$  (determined from experimental data in Ref. 15). Numbers shown against curves represent  $\Omega$ . The broken curve shows the qualitative behavior of the group of terms which correlate with the  $\text{Ne}(4d)$  and  $\text{Ne}(4p')$  states for large  $R$ . The rearrangement of wave functions of the  $\text{He}-\text{Ne}(5s)$  system is localized in the neighborhood of  $R_1$  and  $R_2$ ;  $R_3$ ,  $U_3$  and  $R_4$ ,  $U_4$  are the quasicrossing coordinates.

splitting is of the order of  $10^{-3}$ . We note that the large splitting would prevent the determination of the  $^{1,3}\Sigma^+ \text{He}(2^{1,3}S)$  terms from scattering data. The matrix elements of the interaction between the calculated terms and terms corresponding to other  $\text{Ne}^*$  configurations are also small, since one of the expressions contains the wave function of the highly excited  $s$ -electron, and there is also the interaction between terms corresponding to mostly different ( $\Sigma$  and  $\Pi$ ) states of the quasimolecular ion. This is confirmed by estimates based on the method proposed in Ref. 9, which takes into account core states.

The authors of Ref. 6 have established the presence of groups of attractive terms that correlate for large  $R$  with the  $\text{Ne}(2p^5(^2P_{3/2}^0)3d)$  and  $\text{Ne}(2p^5(^2P_{3/2}^0)4p)$  states ( $3d$ ,  $4p$  terms in Fig. 2), where these states interact with the  $^3\Sigma^+ \text{He}(2^3S_1)$  state. Additional analysis shows that attractive states that interact with both  $^3\Sigma_{1,0}^+ \text{He}(2^3S_1)$  and  $\text{He}-\text{Ne}(ns)$  states are those for which the excited electron is in the  $\sigma 3d$  orbital (this orbital corresponds to attraction after interaction with the analogous state in the  $4p$  group; see Figs. 1 and 2 of Ref. 9), and the ionic core is mostly in the  $\Sigma$ -state. We shall refer to it as the  $^3\Sigma^+ \text{Ne}(3d)$  state.<sup>3)</sup> The other attractive  $\Sigma$ -state,  $^1\Sigma^+ \text{Ne}(3d)$ , does not participate in excitation transfer. The  $3d$ ,  $4p$  potentials determined in Ref. 6 are close to one another in the region in which we are interested, and it will be assumed below that the interaction in the  $^3\Sigma^+ \text{Ne}(3d)$  state is described by the  $3d$  potential<sup>6</sup> (Fig. 2).

$E \cdot 10^3$ , at.un.

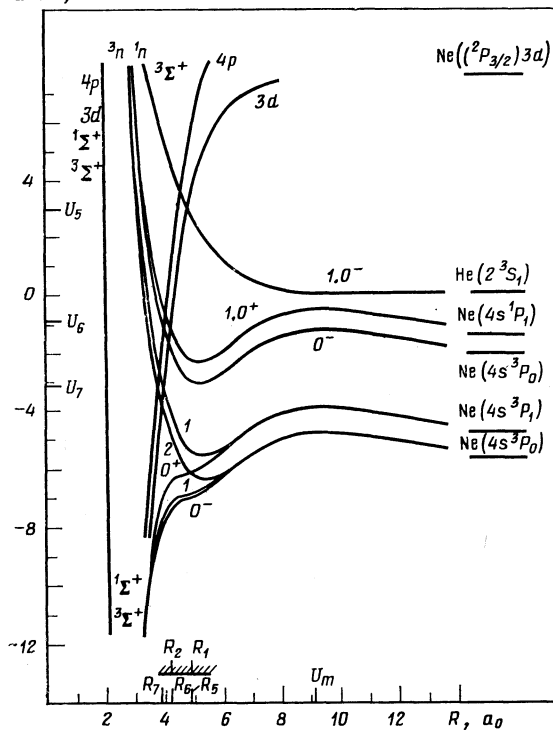


FIG. 2. Quasimolecular terms  $\Omega$   $\text{Ne}(4s^{1.3}P_J)$  (Sec. 2) and  $^3\Sigma^+ \text{He}(2^3S_1)$  determined from experimental data in Ref. 6. The  $3d$  and  $4p$  terms which, for large  $R$ , are correlated with the  $\text{Ne}(3d)$  and  $\text{Ne}(4p)$  states, were established in Ref. 6, and the  $3d$  potential corresponds to interaction in the  $^3\Sigma^+ \text{Ne}(3d)$  state (see Sec. 2). The rearrangement of the wave function of the  $\text{He}-\text{Ne}(4s)$  state is localized in the neighborhood of  $R_1$ ,  $R_2$ ,  $R_5$ ,  $U_5$ ,  $R_6$ ,  $U_6$ , and  $R_7$ ,  $U_7$  are the quasicrossing coordinates.

We note that our calculation of the  $\text{He}-\text{Ne}(ns)$  interaction enables us to calculate the probability of transitions between different  $\text{He}-\text{Ne}(ns)$  terms, the inclusion of which is unimportant for the excitation-transfer processes considered below. The rearrangement of the wave functions of the  $\text{He}-\text{Ne}(ns)$  quasimolecule is localized in the neighborhood of the distances  $R_1$  and  $R_2$  of halfwidth  $\Delta R \approx 0.5$ .

### §3. THE $\text{He}(2^1S_0) + \text{Ne} \rightarrow \text{He} + \text{Ne}(2p^55s)$ EXCITATION TRANSFER

The term picture established in Sec. 2 enables us to conclude that the population of the  $\text{Ne}(5s^{1.3}P_J)$  states in reaction (1) is determined by essentially different mechanisms. Let us begin with the  $^1P_1$  working laser level. The principal contribution to its population is due to transitions to regions of quasicrossing between the  $^1\Sigma_{0+}^+ \text{He}(2^1S_0)$  and  $0^+ \text{Ne}(^1P_1)$  terms. The crossing coordinates are listed in the table. The reasons for the slight influence of the  $1\text{Ne}(^1P_1)$  and  $0^- \text{Ne}(^3P_0)$  terms are discussed below.

To determine the matrix element  $a_3$  of the interaction between the  $0^+$  states in the quasicrossing region, we used experimental data<sup>11,12</sup> on the temperature dependence of the rate constant  $K_4(T)$  for excitation transfer in the reaction



For  $T < 800$  K, we can neglect the transfer of excitation to higher-lying levels<sup>3</sup> of the  $\text{Ne}(2p^54d)$  configuration (see Fig.

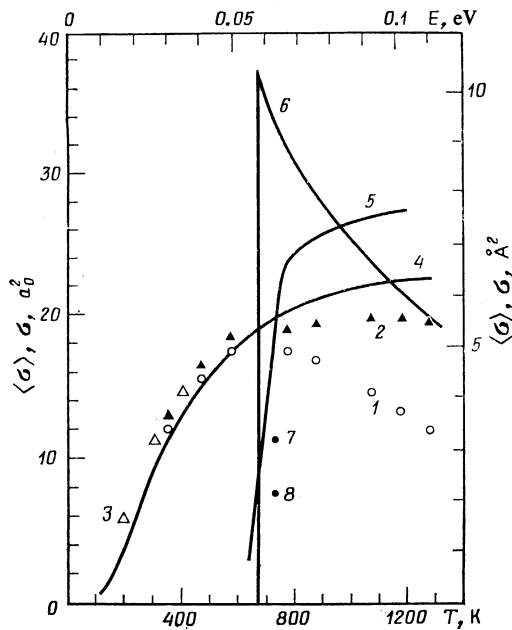


FIG. 3. Excitation transfer cross sections for the  $\text{He}(2^1S_0) + \text{Ne}$  reactions. 1-4—temperature dependence of the cross section averaged over the Maxwellian distribution  $\langle \sigma(T) \rangle = K(T)/\bar{v}$ ; 5-8—energy dependence of the cross section  $\sigma(E)$ . 1—excitation of the  $\text{Ne}(5s^1P_1)$  state, experiment;<sup>11</sup> 2, 3—quenching of the  $\text{He}(2^1S_0)$  state, experiment.<sup>11,12</sup> The uncertainty in the experimental data<sup>11,12</sup> is 30%; 4—excitation of the  $\text{Ne}(5s^1P_1)$  state, calculated from (7); 5—excitation cross section for the  $\text{Ne}(5s^1P_1)$  state, calculated with allowance for orbiting for  $R < R_m$ ; 6—excitation of the  $\text{Ne}(5s^1P_1)$  state, calculated;<sup>20</sup> 7—cross section for the excitation of the  $\text{Ne}(5s^1P_1)$  state,<sup>2</sup> deduced from experimental data on differential scattering within the framework of the optical model; 8—cross section for the excitation of the  $\text{Ne}(5s^1P_1)$  state,<sup>2</sup> calculated by the strong coupling method.

3), so that  $K_4(T)$  can be calculated from the usual Landau-Zener formula,<sup>4</sup> according to which the transition probability is

$$P_3 \left( \frac{\xi_3}{E^{1/2}} \right) = 2p_3(1-p_3),$$

$$p_3 = \exp \left( -\frac{\xi_3}{E^{1/2}} \right), \quad \xi_3 = \frac{2\pi a_3^2}{\Delta F} \left( \frac{\mu}{2} \right)^{1/2}, \quad (5)$$

where  $\Delta F = 1.7 \cdot 10^{-3}$  is the difference between the term strengths. We shall now take into account the fact that the  $0^+ \text{Ne}(^1P_1)$  term has a broad potential barrier for  $R > 8$ , whose height is<sup>5</sup>  $U'_m = 2.3 \times 10^{-4}$  for  $R_m = 10$ , so that, at low energies, the upper limit  $\rho_{\max}(E')$  in the integral with respect to the impact parameter

$$\sigma(^1P_1 \rightarrow ^1S_0 | E') = \frac{1}{3} \int_0^{\rho_{\max}} 2\pi P_3 \rho \, d\rho \quad (6)$$

is determined from the orbiting condition in the attractive part of the potential ( $R < R_m$ ). However, subsequent calculations of the cross section  $\sigma_4(E)$  for the reaction (4) shows that, when the formula for  $K_4(T)$  is derived, we can neglect orbiting and assume that

$$\rho_{\max}(E') = \min \{ R_3(1-U'_3/E')^{1/2}, R_m(1-U'_m/E')^{1/2} \}.$$

As in the case of the crossing of repulsive terms,<sup>17</sup> we can then relate  $K_4(T)$  to the transition probability by a single integration:

$$K_4(T) = \bar{v} \langle \sigma_4(T) \rangle = \bar{v} \frac{\pi R_3^2}{T} \exp \left( -\frac{U_m}{T} \right) \times \left\{ \int_0^{\infty} P_3 \left( \frac{\xi_3}{(U_m - U_3 + E)^{1/2}} \right) \exp \left( -\frac{E}{T} \right) dE \right. \\ \left. + \lambda \int_0^{v_\lambda} P_3 \left( \frac{\xi_3}{(U_m - U_3 - \lambda E)^{1/2}} \right) \exp \left( -\frac{E}{T} \right) dE \right\},$$

$$U_\lambda = (U_m - U_3)/\lambda, \quad \bar{v} = (8T/\pi\mu)^{1/2}, \quad \lambda = R_m^2/R_3^2 - 1. \quad (7)$$

Comparison of (7) with experimental data<sup>11,12</sup> on  $K_4(T)$  for  $T < 800$  K (Fig. 3) has enabled us to establish the value of the only free parameter  $\xi_3$  and hence determine the matrix element  $a_3$  of the interaction (see Table I). The energy dependence of the cross section  $\sigma_4(E)$  for the process (4) is shown in Fig. 3. The results obtained with and without orbiting are close for  $R < R_m$  (they are indistinguishable in the scale of the figure), and this justifies the use of (7).

The attractive nature of the final term in (4) in the quasi-crossing region (i.e.,  $U'_3 < 0$ ), and the reduction in the cross section  $\sigma_4(E)$  as the energy approaches the threshold value, was established in Ref. 3, but only on the basis of an analysis of  $K_4(T)$  with the aid of asymptotic expressions.<sup>18,19</sup> The estimated values of the term interaction parameters given in Ref. 3 are listed in the table. The cross section  $\sigma_4$  was calculated in Ref. 2 by the same coupling method, assuming that  $U'_3 > 0$ . The cross section obtained in this way is much lower than that calculated above (Fig. 3).

The  $\text{He}(2^1S) + \text{Ne}$  elastic and inelastic scattering cross sections have recently been measured<sup>20</sup> in the 25–225 meV region and the data were used to determine the interaction parameters  $R_3$ ,  $U_3$ ,  $a_3$ . The results were in good agreement with the values established above (see Table I). The cross

TABLE I. Parameters of the interaction between the terms  $0^+ \text{Ne}(5s^1P_1)$  and  $^1\Sigma_{0^+} \text{He}(2^1S)$

Parameter;	Present work;	Data from Ref. 3;	Data from Ref. 20;
$R_3$	5.8	6.4	5.74
$U_3$	$1.2 \cdot 10^{-3}$	$4.4 \cdot 10^{-4}$ *	$1.4 \cdot 10^{-3}$
$\xi_3$	0.01	$3.6 \cdot 10^{-3}$	
$a_3$	$2.2 \cdot 10^{-4}$	$> 8 \cdot 10^{-5}$	$2.1 \cdot 10^{-4}$

\*The value  $U_0 = -1.32 \times 10^{-3}$ , established in Ref. 3, was measured from the  $\text{Ne}(5s^1P_1)$  state and not from  $\text{He}(2^1S_0)$ , as erroneously pointed out in Ref. 3.

section  $\sigma_4(E)$  for process (4), calculated in Ref. 20 from these values of the interaction parameters (Fig. 3), is found to reach a maximum at the reaction threshold and decrease with increasing energy. This is essentially different from the threshold dependence of the cross sections established above in the presence of the potential barrier, the existence of which was noted in Ref. 20 as well:

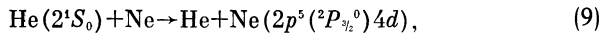
$$\sigma_4(E) \rightarrow \pi R_m^2 \frac{E - U_m}{E} P_3 \left( \frac{\xi_3}{(U_m - U_3)^{1/2}} \right). \quad (8)$$

The small difference between the threshold energies (curves 5 and 6 in Fig. 3) is due to the fact that the value  $U_m = 4 \times 10^{-4}$  adopted in Ref. 20 is greater than the result  $U'_m(R_m = 10) = 2.3 \cdot 10^{-4}$  calculated in Sec. 2. Moreover, it was assumed in Ref. 20 that the former value was reached in the region of the external maximum of the  $5s$ -electron wave function ( $R_m \approx 20$ ). The term calculations of Sec. 2 indicate that this region does, in fact, contain a potential barrier, but its height is much lower than the barrier height at  $R_m = 10$ .

Let us now consider the effect of other terms on the quenching of the  $\text{He}(2^1S_0)$  state and the population of  $\text{Ne}(^1P_1)$ . A Coriolis transition between the  $0^+(^1P_1)$  and  $1(^1P_1)$  terms is possible for  $R < R_3$ . Inclusion of this transition leads to an increase in the probability  $P_3$  in (7) by the amount  $(1 - p_3)^2 \sin^2 \Phi$  (see, for example, Ref. 21), where  $\Phi$  is the angle of rotation of the molecular axis when the region  $R < R_3$  is traversed. Since  $p_3 \approx 0.8$ , the influence of this transition can be neglected.

It is clear from the term diagram (Fig. 1) that the  $\text{Ne}(5s^3P_0)$  level is not populated in single collisions because the selection rule forbids transitions between the  $0^+$  and  $0^-$  states, and this is in agreement with experiment.<sup>22</sup> This ensures that, at  $T = 360$  K, the excitation constant for this state is lower by a factor of 400 than the constant for process (4). The small population of the  $\text{Ne}(5s^3P_0)$  level, reported in Ref. 22, is probably due to multiple collisions.

For  $T > 800$  K, there is a discrepancy between the measured values of  $K_4(T)$  and the calculations based on (7) (Fig. 3). It was noted in Ref. 3 that population of  $\text{Ne}(4d)$  levels may be the reason for this discrepancy at these temperatures. Detailed examination based on an analysis of the simultaneous population of the  $\text{Ne}(5s^1P_1)$  and  $\text{Ne}(4d)$  states and the use of rate data<sup>11</sup> for the process



shows that, for  $T \geq 500$  K, the correction to (7) due to transitions to the  $4d$  terms in the region of quasicrossing between the  $^1\Sigma^+ \text{He}(2^1S)$  term and the  $0^+ \text{Ne}(4d)$  terms near  $R_4$  is  $\langle \Delta\sigma_4 \rangle \approx -1$  and cannot explain the discrepancy between theory and experiment. The basic reason for the discrepancy can be established by noting that, for  $T \gtrsim 800$  K, the calculated  $\text{Ne}(5s^1P_1)$  population constant is equal to within the limits of uncertainty with the experimental quenching constant of  $\text{He}(2^1S_0)$ . For characteristic transition probability values  $p_3, p_4 \sim 1$ , where  $p_4$  is the probability of diabatic passage through the quasicrossing region near  $R_4$  in Fig. 1 between the term  $^1\Sigma_{0+}^+ \text{He}(2^1S_0)$  and the terms  $0^+ \text{Ne}(4d)$ , this situation may occur when there is a substantial outflow directly from the  $0^+ \text{Ne}(5s^1P_1)$  term in the region of sufficiently large

values of  $U_{0+} \approx 4 \cdot 10^{-3}$  for  $R < R_3$  to terms that are correlated with the higher-lying neon states, for example, the  $4d, 4f$  states. The  $\text{He}(2^1S_0)$  quenching probability is then  $2(1 - p_3)$ , and is approximately equal to the  $\text{Ne}(5s^1P_1)$  population probability calculated above without taking into account the transitions for  $R < R_3$ .

The population of the  $\text{Ne}(5s^3P_1, ^3P_2)$  states is due to double quasicrossings (Fig. 1). The experimental values of the cross sections  $\langle \sigma(T) \rangle$  for these processes are lower by an order of magnitude as compared with the cross section<sup>22</sup>  $\langle \sigma_4(T) \rangle$ , which is natural for the characteristic values of transition probabilities  $p \approx 0.8 - 0.9$ .

#### §4. $\text{He}(2^3S_1) + \text{Ne} \rightarrow \text{He} + \text{Ne}(2p^54s)$ EXCITATION TRANSFER

The term picture established in Sec. 2 (Fig. 2) enables us to conclude that the basic mechanism responsible for the  $\text{He}(2^3S_1) \rightarrow \text{Ne}(2p^54s)$  excitation transfer is as follows.

In the course of a collision, excitation is transferred from  $\text{He}(2^3S_1)$  initially to an intermediate term during the quasicrossing of the terms  $^3\Sigma^+ \text{Ne}(2^3S_1)$  and  $^3\Sigma^+ \text{Ne}(3d)$  for  $R_5 = 4.9$  and  $U_5 = 2.95 \times 10^{-3}$ . The  $\text{Ne}(4s^1P_1, ^3P_0)$  state is populated as a result of the quasicrossing of the terms  $^3\Sigma_1^+ \text{Ne}(3d)$  with  $1\text{Ne}(4s^1P_1)$  and  $^3\Sigma_{0-}^+ \text{Ne}(3d)$  with  $0^- \text{Ne}(4s^3P_0)$  at  $R \approx R_6 = 4.2$ . The terms  $1\text{Ne}(4s^3P_1)$  and  $2\text{Ne}(4s^3P_2)$  do not interact with the intermediate term  $^3\Sigma^+$  because, for these terms, calculations show that a complete rearrangement has taken place near  $R_1 = 4.9$ , and for  $R \approx R_7 = 4.0$  the ion core is in the  $\Pi$  state. For the  $1, 0^+ \text{Ne}(^1P_1)$  and  $0^- \text{Ne}(^3P_0)$  states, this remark is not valid because these states are similar to the  $1, 0^- \text{Ne}(^3P_2)$ ,  $0^+ \text{Ne}(^3P_1)$  states in that rearrangement occurs near  $R_2 = 4.2$ , and the admixture of the ionic  $\Sigma$ -state in the crossing region at  $R \approx R_6 = 4.2$  is considerable. Thus, the population of the  $\text{Ne}(4s^3P, ^3P_2)$  states is small in comparison with  $\text{Ne}(4s^3P_0, ^1P_1)$ . The above qualitative difference between the populations of the  $\text{Ne}(4s^1P_1, ^3P_0)$  and  $\text{Ne}(4s^3P_1, ^3P_2)$  states is in agreement with experimental data.<sup>23,24</sup> We note that the importance of the intermediate terms for the population of the  $\text{Ne}(4s)$  states was first mentioned in Ref. 6.

We now proceed to the determination of the temperature dependence of the rate constant, since comparison of this function with experimental data will enable us to establish values of the remaining parameters and to calculate the energy dependence of the cross section. The difficulty encountered here is that it is essential to take into account the vibrational nature of the motion of the atoms in the diabatic potential corresponding to  $^3\Sigma^+ \text{Ne}(3d)$  and the adiabatic potentials produced when this term crosses the  $^3\Sigma^+ \text{He}(2^3S_1)$  and  $1, 0^- \text{Ne}(4s^1P_1, ^3P_0)$  terms. (In the discussion given below, the  $1, 0^- \text{Ne}(^1P_1, ^3P_0)$  terms, the splitting for which is  $\Delta E \approx 8 \cdot 10^{-4}$ , are looked upon as a single term.) In the region of the crossing  $R_5, U_5$ , thermal collisions are characterized by action  $S \leq 1$ , so that a quantum-mechanical analysis of the motion of the atoms that takes into account the interference character of the transitions during repeated crossing of the region is essential. Let  $\Gamma$  be the probability of the nonadiabatic crossing  $^3\Sigma^+ \text{He}(2^3S_1) \rightarrow ^3\Sigma^+ \text{Ne}(3d)$  that satisfies this condition.

The action between  $R_5$ ,  $U_5$  and  $R_6$ ,  $U_6$  is  $S \approx 5$ , so that, in this region, the motion of the atoms may be treated classically, and we can sum the usual Landau-Zener probabilities of the  $P$ -transition  ${}^3\Sigma^+ \text{Ne}(3d) \rightarrow 1,0^- \text{Ne}({}^1P_1, {}^3P_0)$  for each vibration independently. This approach yields

$$W = \Gamma P / (\Gamma + P - \Gamma P), \quad (10)$$

so that  $W$  is approximately equal to the smaller of the two quantities  $\Gamma$  and  $P$ . We note that the Landau-Zener transitions were examined in Refs. 25 and 26 with allowance for multiple vibrations in the effective potential well and passage through the centripetal barrier. Both the quantum mechanical and semiclassical approaches were used. The formula obtained in these papers for the transition probability averaged over fast vibrations, i.e., near the top of the centripetal barrier (where the separation between vibrational levels is comparable with the width), differs from (10) in that it does not contain the term  $\Gamma P$  in the denominator, which is small under the conditions assumed in Refs. 25, 26.

Scattering data<sup>6</sup> indicate that there is weak coupling between the diabatic states in the crossing regions, so it is reasonable to suppose that the matrix element  $a_5$  of the interaction between the  ${}^3\Sigma^+ \text{He}(2^3S_1)$  and  ${}^3\Sigma^+ \text{Ne}(3d)$  states is small at  $R = R_5$  and we can use the perturbation-theory formula<sup>27</sup>

$$\Gamma(E_r - U_5) = \pi^2 \beta^{4/3} |\text{Ai}(-\varepsilon \beta^{3/6})|^2, \quad (11)$$

$$\beta = 4a_5 (\mu a_5 / \bar{F} \Delta F)^{1/2},$$

$$\varepsilon = (E_r - U_5) \Delta F / 2a_5 \bar{F}, \quad E_r = E(1 - \rho^2 / R_5^2),$$

for  $\Gamma \ll 1$ , where  $\Delta F = |F_1 - F_2| = 6 \cdot 10^{-3}$ ,  $\bar{F} = |F_1 F_2|^{1/2} = 2.8 \cdot 10^{-3}$  and  $E_r - U_5$  is the radial kinetic energy of the atoms. The terms given in Ref. 6 were used to estimate the strengths  $F_1$ ,  $F_2$ . For large values of  $\Gamma$ , the expression given by (11) is no longer valid, but an exact  $\Gamma$  is not, in fact, required in this region because  $W \approx P$  for  $\Gamma \gtrsim P$ . Moreover, for  $T \lesssim 300$  K, such values of  $\Gamma$  occur in (10) on the tail of the Maxwell velocity distribution.

When the rate constant  $K_2$  ( $T \lesssim 300$  K) for excitation transfer to the  $1,0^- \text{Ne}(4s^1P_1, {}^3P_0)$  levels is calculated from (10) and (11), it is important to remember that  $P$  is a slowly-varying function of the collision energy ( $T \ll U_5 - U_6$ ) and we

may suppose that  $P = \text{const}$ . Moreover, the coordinates  $R_5$  and  $R_6$  are close to one another ( $R_5 - R_6 \ll R_5$ ), so that  $K_2(T)$  can again be related to

$$W(E) = P \Gamma(E) / (\Gamma(E) + P - P \Gamma(E)),$$

by a single integral, namely,

$$K_2(T) = \bar{v} \langle \sigma_2(T) \rangle = \bar{v} \frac{\pi R_5^2}{T} \int_0^\infty W(E - U_5) \exp\left(-\frac{E}{T}\right) dE. \quad (12)$$

The correction to (12) that represents the dependence of  $P$  on the collision energy and the difference between  $R_5$  and  $R_6$  does not exceed  $0.1K_2$  in these cases. Comparison to (12) with experimental data<sup>4</sup> on  $K_2(T)$  (Fig. 4) in the range  $178 \text{ K} \leq T \leq 300 \text{ K}$  has enabled us to estimate the interaction as  $a_5 = 4 \cdot 10^{-4}$  and  $P = 0.25$ . Calculations have shown that the main contribution to the  $\text{Ne}(4s^1P_1, {}^3P_0)$  level population is due to collisions with energies in the range  $0.8 U_5 < E < U_5 + T$ , so that the terms may be assumed to be linear in the subbarrier region when  $K_2(T)$  is calculated. The value  $P = 0.25$  corresponds to  $\xi_6 = 0.01$  and  $a_6 = 5.5 \cdot 10^{-4}$  for the matrix element of the interaction between the  ${}^3\Sigma_{1,0}^+ \text{Ne}(3d)$  and  $1,0^- \text{Ne}(4s^1P_1, {}^3P_0)$  terms. Calculations based on the method put forward in Ref. 9, augmented by the inclusion of the ion core states, have enabled us to estimate the matrix elements between different terms with the same  $\Omega$  in this quasicrossing region. The resulting values of the matrix elements are equal, and are in agreement with the above value of the effective matrix element,<sup>6</sup> so that the  $\text{Ne}(4s^1P_1)$  and  $\text{Ne}(4s^3P_0)$  states are populated in the ratio of 2:1 during the excitation transfer process, which this is in agreement with experimental data<sup>23</sup> that indicate a ratio of 1.7:1.

The energy dependence of the cross section for excitation transfer, calculated for the above parameter values, is shown in Fig. 4. Calculations have shown that the function  $\bar{F}(\rho)$  need not be taken into account. We note that there is a discrepancy, exceeding the experimental uncertainty for  $T > 500$  K, between the calculated  $\langle \sigma_2(T) \rangle$  and experimental data<sup>28</sup> (Fig. 4). The experimental data<sup>28</sup> refer, strictly speaking, to the quenching of the  $\text{He}(2^3S_1)$  state. It follows from the term diagram and the discussion at the beginning of this section that, for  $T < 500$  K, quenching is due to excitation transfer to the  $\text{Ne}(4s^1P_1, {}^3P_0)$  levels. The population of the

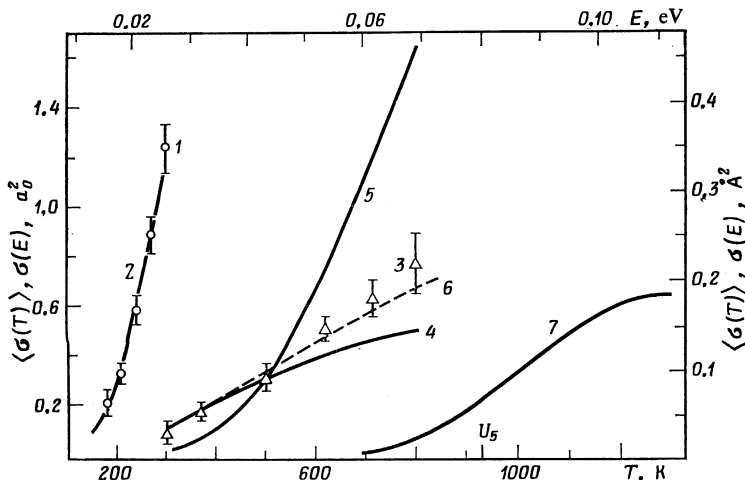
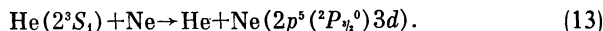


FIG. 4. Excitation transfer cross section for the  $\text{He}(2^3S_1) + \text{Ne}$  reaction: 1-6 — temperature dependence of the cross sections  $\langle \sigma(T) \rangle = K(T) \bar{v}$  averaged over the Maxwell distribution; 7 — energy dependence of the cross section,  $\sigma(E)$ . 1 — quenching of  $\text{He}(2^3S_1)$ , experiment<sup>4</sup>; 2 — excitation of  $\text{Ne}(4s^1P_1, {}^3P_0)$ , calculated from (12); 3 — quenching of  $\text{He}(2^3S_1)$ , experiment<sup>28</sup>,  $\langle \sigma(T) \rangle / 10$ ; 4 — same as 2 but  $\langle \sigma(T) \rangle / 10$ ; 5 — excitation of  $\text{Ne}(2p^5(^2P_{3/2}^o)3d)$ , calculated; 6 — total excitation of  $\text{Ne}(4s^1P_1, {}^3P_0)$  and  $\text{Ne}(2p^5(^2P_{3/2}^o)3d)$ , calculated,  $\langle \sigma(T) \rangle / 10$ ; 7 — excitation of  $\text{Ne}(4s^1P_1, {}^3P_0)$ , calculated,  $\sigma(E) / 10$ , the  ${}^1P_1$  and  ${}^3P_0$  states are populated in the ratio of 2 to 1.

higher-lying neon levels begins as the temperature increases:



It is precisely this reaction that is responsible for the difference in Fig. 3 between curve 4 and points 3. Since the interaction parameters are known, we can calculate the rate constant for reaction (13), and this is indicated by curve 5 in Fig. 4. These calculations include transitions from the  $^3\Sigma^+ \text{Ne}(3d)$  term to the He-Ne( $4s$ ) terms, and orbiting during motion in the  $^3\Sigma^+ \text{Ne}(3d)$  potential. The calculated resultant rate constant  $K(T)$  for reactions (2) and (13) is in good agreement with experimental data (curve 6 and points 3 in Fig. 4).

Next, let us examine the other published suggestions as to the mechanism responsible for reaction (2). The experimental data on  $K(T)$  for reaction (2) were analyzed in Ref. 4 by using the usual relation for exothermal reactions, namely,  $K(T)/\bar{v} = \langle \sigma(T) \rangle = \sigma(E = T)$ , and it was concluded that the population of the Ne( $4s^1P_1, ^3P_0$ ) levels could not be explained within the framework of the Demkov model. For a reasonable value of the model parameter proposed in Ref. 4 ( $\alpha \simeq 1$ ), collisions are almost adiabatic in character at thermal energies and

$$\sigma(E) \propto \exp(-\xi), \quad \xi = \pi \Delta E \mu^{1/2} / \alpha (2E)^{1/2},$$

where  $\Delta E$  is the reaction defect. It is well known<sup>29</sup> that the constant  $K(T)$  is then determined by the tail of the Maxwellian distribution:  $\langle \sigma(T) \rangle \propto \exp(-c/T^{1/3})$  and  $\langle \sigma(T) \rangle \gg \sigma(E = T)$  as can be clearly seen in Fig. 4 (curves 2, 4, and 7). In other words, if we use the energy dependence of the cross section proposed in Ref. 4 to calculate the rate constant, the resulting values of  $K(T)$  turn out to be substantially higher than the experimental values.

Analysis of experimental data on  $K(T)$ , made in Ref. 5 on the basis of the formulas given in Refs. 18 and 30, has shown that the population of the Ne( $4s$ ) levels is due to quasicrossing of the original  $^3\Sigma^+ \text{He}(2^3S_1)$  term with another term in the repulsive region, but it was assumed that the second term was correlated with the Ne( $4s$  state). Of course, the presence of the second quasicrossing, which plays a much smaller role in the temperature dependence  $K(T)$  could not have been established as a result of the comparison with the formulas for  $K(T)$  given in Refs. 18 and 13 because they take into account the presence of only one nonadiabatic region. This can be done only by introducing additional experimental data, as in Ref. 6, where the simultaneous population of the Ne( $4s$ ) and Ne( $3d$ ) levels was established, or by introducing additional theoretical considerations, i.e., by constructing the quasimolecular term diagram.

## §5. CONCLUSION

The quasimolecular term scheme constructed on the basis of elastic scattering data and additional theoretical ideas, and comparison of experimental data on  $K(T)$  with calculations, have enabled us to determine the parameters of the nonadiabatic interaction that determines the transfer of excitation in the helium-neon laser. This comparison turns out to be fruitful because we have been able to relate  $K(T)$  to the required parameters without using the energy dependence of the cross section. The function  $\sigma(E)$  calculated from

the resulting parameter values may turn out to be useful, for example, in optimizing nontraditional He-Ne laser schemes such as plasma, gas-dynamic, and so on, systems. This way of obtaining the energy dependence of the excitation transfer cross sections will be useful in other cases, since it enables us to combine studies of elastic scattering of beams with the relative simplicity of measuring  $K(T)$  for inelastic processes in plasmas and gas discharges.

The basic conclusions of this work on the population of the He-Ne laser levels are as follows. The population of the Ne( $5s^1P_1$ ) state occurs as a result of Landau-Zener quasicrossing of terms corresponding to the initial and final states. The population of the Ne( $4s^1P_1$ ) level is accomplished by the quasicrossing of terms corresponding to the initial and final states with an intermediate term. Subbarrier transitions take place in this reaction for temperatures  $T \leq 300$  K.

The authors are greatly indebted to Yu. N. Demkov and N. P. Penkin for useful discussions.

<sup>1</sup>There are no reliable published methods for calculating this quantity in the case of excitation transfer processes.

<sup>2</sup>This notation represents the term that correlates with the He( $2^1S$ ) level for  $R \rightarrow \infty$ . For states correlating with He-Ne( $ns$ ), we give the number  $\Omega$  and the state of the Ne( $ns$ ) atom which, for brevity, is indicated in the  $LS$ -coupling notation.

<sup>3</sup>The final rearrangement of the wave functions is completed for  $R \leq 5$  in the case of Hund type  $a$ .

<sup>4</sup>The Zener formula is justified because the  $0^+ \text{Ne}(^1P_1)$  term strength is small in the quasicrossing region (Ref. 16).

<sup>5</sup>Primed energy variables are measured from the final state as  $R \rightarrow \infty$ , in this case, from He-Ne( $5s^1P_1$ ).

<sup>1</sup>B. M. Smirnov, Vosbuzhdennye atomy (Excited Atoms), Energoizdat, Moscow, 1982, p. 91.

<sup>2</sup>P. E. Siska and T. Fukuyama, Tenth Intern. Conf. Phys. Electron. Atom. Collisions, Abstract of Papers, Paris, 1977, p. 552.

<sup>3</sup>A. K. Belyaev, A. Z. Devdariani, V. A. Kostenko, and Yu. A. Tolmachev, Opt. Spektrosk. **49**, 633 (1980) [Opt. Spectrosc. (USSR) **49**, 345 (1980)].

<sup>4</sup>R. A. Zhitnikov, V. A. Kartoshkin, G. V. Klement'ev, and V. D. Mel'nikov Zh. Eksp. Teor. Fiz. **80**, 992 (1981) [Sov. Phys. JETP **53**, 504 (1981)].

<sup>5</sup>A. K. Belyaev and A. Z. Devdariani, Opt. Spektrosk. **53**, 610 (1982) [Opt. Spectrosc. (USSR) **53**, 362 (1982)].

<sup>6</sup>H. Haberland and P. Z. Oesterlin, Z. Phys. A **304**, 11 (1982).

<sup>7</sup>E. E. Nikitin and M. Ya. Ovchinnikova, Usp. Fiz. Nauk **104**, 379 (1971) [Sov. Phys. Usp. **14**, 394 (1972)].

<sup>8</sup>G. K. Ivanov, Teor. Eksp. Khim. **14**, 610 (1978).

<sup>9</sup>G. K. Ivanov, Teor. Eksp. Khim. **15**, 644 (1979).

<sup>10</sup>I. Dabrowski and G. Herzberg, J. Mol. Spectrosc. **73**, 183 (1978).

<sup>11</sup>V. A. Kostenko and Yu. A. Tolmachev, Opt. Spektrosk. **47**, 1050 (1979) [Opt. Spectrosc. (USSR) **47**, 582 (1979)].

<sup>12</sup>C. R. Jones, F. E. Niles, and W. W. Robertson, J. Appl. Phys. **40**, 3967 (1969).

<sup>13</sup>D. L. Cooper, J. Chem. Phys. **76**, 6443 (1982).

<sup>14</sup>E. E. Nikitin, Opt. Spektrosk. **19**, 161 (1965) [Opt. Spectrosc. (USSR) **19**, 91 (1965)].

<sup>15</sup>C. H. Chen, H. Haberland, and Y. T. Lee, J. Chem. Phys. **61**, 3095 (1974).

<sup>16</sup>M. Ya. Ovchinnikova, Opt. Spektrosk. **17**, 822 (1964) [Opt. Spectrosc. (USSR) **17**, 447 (1964)].

<sup>17</sup>E. E. Nikitin and V. K. Bykhovskii, Opt. Spektrosk. **17**, 815 (1964) [Opt. Spectrosc. (USSR) **17**, 444 (1964)].

<sup>18</sup>A. K. Belyaev and A. Z. Devdariani, Opt. Spektrosk. **45**, 448 (1978) [Opt. Spectrosc. (USSR) **448**, 253 (1978)].

<sup>19</sup>A. Z. Devdariani, Opt. Spektrosk. **47**, 106 (1979) [Opt. Spectrosc. (USSR) **47**, 58 (1979)].

<sup>20</sup>H. Haberland, W. Konz, and P. Oesterlin, J. Phys. B. **15**, 2969 (1982).

<sup>21</sup>A. Z. Devdariani and A. L. Zagrebini, Khim. Fiz. **8**, 1141 (1982).

<sup>22</sup>Yu. Z. Ionikh and N. P. Penkin, Opt. Spektrosk. **31**, 837 (1971) [Opt. Spectrosc. (USSR) **31**, 453 (1971)].

- <sup>23</sup>I. M. Beterov and V. P. Chebotaev, *Opt. Spektrosk.* **20**, 1078 (1966) [*Opt. Spectrosc. (USSR)* **20**, 597 (1966)].
- <sup>24</sup>S. T. Massey, A. G. Schulz, B. F. Hochheimer, and S. M. Cannon, *J. Appl. Phys.* **36**, 658 (1965).
- <sup>25</sup>T. A. Vartanyan and S. G. Przhibel'skiĭ, *Zh. Eksp. Teor. Fiz.* **74**, 1579 (1978) [*Sov. Phys. JETP* **47**, 824 (1978)].
- <sup>26</sup>T. A. Vartanyan and S. G. Przhibel'skiĭ, *Opt. Spektrosk.* **45**, 433 (1978) [*Opt. Spectrosc. (USSR)* **45**, 245 (1978)].
- <sup>27</sup>E. E. Nikitin and S. Ya. Umanskiĭ, *Nadiabaticheskie perekhody pri medlennykh atomnykh stolknovennykh (Nonadiabatic Transitions in Slow Atomic Collisions)*, Atomizdat, Moscow, 1979, p. 193.
- <sup>28</sup>W. Lindinger, A. L. Schmeltekopf and F. C. Fehsenfeld, *J. Chem. Phys.* **61**, 2890 (1974).
- <sup>29</sup>L. Landau and E. Teller, *Phys. Z. Sowjetunion* **10**, 34 (1936).
- <sup>30</sup>A. K. Belyaev, A. Z. Devdariani, and A. L. Zagrebin, *Opt. Spektrosk.* **53**, 807 (1982) [*Opt. Spectrosc. (USSR)* **53**, 481 (1982)].

Translated by S. Chomet